Long non-coding RNA *H19* regulates viability and metastasis, and is upregulated in retinoblastoma

LI LI[1], WEI CHEN[1], YUCHUAN WANG[1], LUOSHENG TANG[2] and MEI HAN[1]

[1]Department of Vitreous and Retinal Diseases, Clinical College of Ophthalmology of Tianjin Medical University, Tianjin 300020; [2]Department of Ophthalmology, The Second Affiliated Hospital of Xiangya Medical College, Central-South University, Changsha, Hunan 410083, P.R. China

Received July 21, 2016; Accepted November 16, 2017

DOI: 10.3892/ol.2018.8385

Abstract. Retinoblastoma is the most common type of intraocular pediatric malignant tumor, which typically affects children <6 years of age. However, the underlying molecular mechanisms of retinoblastoma progression remain unclear. The aim of the present study was to investigate the function of long non-coding RNA (lncRNA) *H19* in retinoblastoma clinical samples and cell lines, using reverse transcription-quantitative polymerase chain reaction, western blotting, colony formation, MTT, fluorescence activated cell sorting, cell invasion and migration, and *in vivo* growth assays. The results demonstrated that *H19* may serve a critical oncogenic function in the progression of retinoblastoma, as lncRNA *H19* levels were markedly increased in retinoblastoma cells and tissues compared with corresponding controls. In addition, patients with retinoblastoma with increased lncRNA *H19* expression experienced poorer survival time compared with those with decreased lncRNA *H19* levels. Knockdown of lncRNA *H19* significantly suppressed retinoblastoma cell proliferation, migration and invasion *in vitro* and *in vivo*. Furthermore, lncRNA *H19* expression was also associated with multiple proteins, including cyclin-dependent kinase 1, B-cell lymphoma-associated X protein, apoptosis regulator, tumor protein p53, vimentin, cadherin 13 and matrix metallopeptidase 9. In conclusion, lncRNA *H19* may serve an important function in tumorigenesis and may be a potential target for therapy and prognosis in retinoblastoma.

Introduction

Retinoblastoma is a type of embryonic malignant tumor of the retina of the eye, which originates from primitive stem cells (1). Retinoblastoma primarily occurs in childhood, with an average incidence of between 1/15,000 and 1/20,000 live births, typically arising in infants <6 years of age, often prior to the age of 2 years (2). Advanced retinoblastoma is able to rapidly cover the eye, invade the optic nerve and eventually spread to the central nervous system. Previous evidence from molecular, cellular and cytogenetic studies has indicated that retinoblastoma is typically caused by a mutation in the RB transcriptional co-repressor 1 (*RB1*) gene on chromosome 13 (3-5). *RB1* inactivation results in mitotic defects, contributing to genomic instability, which manifests as aneuploidy and chromosomal rearrangements (6,7). At present, non-metastatic retinoblastoma is not considered a fatal childhood cancer and is effectively treated by enucleation, dependent on an early diagnosis and accurate prognosis of the disease (8). Dalgard *et al* (9) observed that the retinoblastoma cell lines Y79 and Weri-Rb1, and retinoblastoma tumor samples, presented with aberrant microRNA (miR)-34a and miR-34b expression. In addition, this study provided indicated that knockdown of miR-34a may result in increased retinoblastoma cell proliferation and chemotherapeutic resistance.

The aim of the present study was to investigate long non-coding RNA (lncRNA) *H19*-mediated regulation of the development of retinoblastoma in clinical samples and cell lines. LncRNAs are non-protein-coding transcripts, which are >200 nucleotides in length, and regulate gene expression transcriptionally or post-transcriptionally. These intergenic transcripts are involved in diverse cellular processes, including proliferation, migration, invasion, apoptosis and the reprogramming of stem cell pluripotency (10-13). LncRNA *H19* has been considered as an oncogenic lncRNA in multiple types of cancer, including hepatocellular, bladder carcinoma, breast cancer, bladder tumor and glioma (14-17). Furthermore, previous studies reported that *H19* regulates the development of gliomas via interactions with miR-675, which in addition contributes to the proliferation of gastric cancer cells and was associated with tumor metastasis (18-20). Emerging evidence has also demonstrated that *H19* expression is upregulated, and is involved, in carcinogenesis and cancer metastasis via the promotion of cell cycle progression (21). However, the function of *H19* in retinoblastoma remains unclear.

In the present study, the clinical characteristics, biological function and potential underlying molecular mechanisms of lncRNA *H19* in retinoblastoma were investigated. The

Correspondence to: Dr Mei Han, Department of Vitreous and Retinal Diseases, Clinical College of Ophthalmology of Tianjin Medical University, 4 Gansu Road, Tianjin 300020, P.R. China
E-mail: hanmeimei1968@163.com

Key words: long non-coding RNAs, *H19*, retinoblastoma

results indicated that *H19* levels were markedly increased in retinoblastoma cells and tissues. Furthermore, patients with retinoblastoma with increased lncRNA *H19* expression experienced poorer survival time compared with patients with lower levels of lncRNA *H19* expression. Furthermore, lncRNA *H19* expression was also associated with several proteins, including cyclin-dependent kinase 1 (CDK1), B-cell lymphoma 2-associated X, apoptosis regulator (Bax), tumor protein p53 (p53), vimentin, cadherin 13 (CDH13) and matrix metalloproteinase 9 (MMP9). The oncogenic function of *H19* suggests that it may serve as a potential target for retinoblastoma therapy and prognostic prediction.

Materials and methods

Cell lines and tumor tissues. The present study was approved by the Research Ethics Committee of Tianjin Eye Hospital (Tianjin, China). Written informed consent for all biological procedures was obtained from each patient, or their parents, and specimens for the present study were anonymized. Patients who had received treatment prior to surgery were excluded from the present study. The tumor samples were collected between June 2011 until November 2015 and were extracted from enucleated eyes and immediately snap-frozen in liquid nitrogen and stored at -80˚C. A total of 80 freshly frozen retinoblastoma tissue samples (44 males and 36 females; the age distribution: 40 patients ≥2 years and 40 patients <2 years), and five normal retina samples (3 males and 2 females; the age distribution: 2 patients ≥2 years and 3 patients <2 years) obtained from ruptured globes, were collected at Tianjin Eye Hospital (Tianjin, China).

Cell culture. The cell lines used in the present study were purchased from the Institute of Biochemistry and Cell Biology of the Chinese Academy of Sciences (Shanghai, China). The human retinal pigment epithelial cell line ARPE-19 was cultured in Dulbecco's modified Eagle's medium (Gibco; Thermo Fisher Scientific, Inc., Waltham, MA, USA) supplemented with 10% fetal bovine serum (FBS; Gibco; Thermo Fisher Scientific, Inc.), 100 U/ml penicillin (Invitrogen, Thermo Fisher Scientific, Inc.), and 100 mg/ml streptomycin (Invitrogen, Thermo Fisher Scientific, Inc.). The human retinal microvascular endothelial cell line (HRMEC) was maintained in Endothelial-Cell Growth medium (EGM-2 SingleQuot Kit Supplement & Growth Factors; Lonza Group, Ltd., Basel, Switzerland), supplemented with 10% fetal bovine serum (FBS; Gibco; Thermo Fisher Scientific, Inc.), 100 U/ml penicillin (Invitrogen, Thermo Fisher Scientific, Inc.), and 100 mg/ml streptomycin (Invitrogen, Thermo Fisher Scientific, Inc.). The retinoblastoma cell lines Weri-Rb1 and Y79 were maintained in RPMI-1640 medium (Gibco; Thermo Fisher Scientific, Inc.) supplemented with 10% FBS, 100 U/ml penicillin (Invitrogen, Thermo Fisher Scientific, Inc.), and 100 mg/ml streptomycin (Invitrogen, Thermo Fisher Scientific, Inc.). All cell cultures were incubated at 37˚C in a humidified atmosphere containing 5% CO_2.

RNA extraction and reverse transcription-quantitative polymerase chain reaction (RT-qPCR). Total RNA was extracted using TRIzol reagent (Invitrogen; Thermo Fisher Scientific, Inc.), according to the manufacturer's protocol. RNA was purified and then reverse-transcribed into cDNA using a PrimeScript RT Reagent kit (Takara Biotechnology Co., Ltd., Dalian, China) according to the manufacturer's protocol. qPCR was performed using SYBR Premix Ex Taq (Takara Biotechnology Co., Ltd.), according to the manufacturer's protocol, and run on an ABI Prism 7000 Sequence Detection System. Relative expression of lncRNA *H19* (primer: Forward, 5'-ATCGGTGCCTCAGCGTTCGG-3'; and reverse, 5'-CTG TCCTCGCCGTCACACCG-3) was normalized to the expression of GAPDH (primer: Forward, 5'-AGCCACATCGCTCAG ACAC-3' and reverse, 5'-GCCCAATACGACCAAATCC-3'). Relative gene expression levels were quantified using the $2^{-\Delta\Delta Cq}$ method (22). The thermocycling conditions for lncRNA *H19* quantification were as follows: 95˚C for 10 min; 40 cycles of 95˚C for 15 sec and 60˚C for 1 min. Each sample was examined in triplicate.

Small interfering (si)RNA transfection. RNA interference was conducted using synthetic siRNA duplexes. Two synthetic siRNA duplexes (si-H19) corresponding to the *H19* mRNA sequences, 5'-CCCACAACAUGAAAGAAAU-3' (forward) and 5'-GCUAGAGGAACCAGACCUU-3' (reverse), were used to inhibit *H19* RNA expression. si-H19 and si-negative control (NC) were purchased from Guangzhou RiboBio Co., Ltd. (Guangzhou, China). Cells were cultured in 6-well plates and maintained until they reached ~60% confluence, prior to transfection with siRNA duplexes (25 nM) using Lipofectamine® 2000 (Invitrogen; Thermo Fisher Scientific, Inc.), according to the manufacturer's protocol. Transfection efficiency to assess the inhibition of *H19* after 48 h of transfection in Y79 cells was performed using RT-qPCR as previously outlined.

Flow cytometric analysis. Cell apoptosis was examined by flow cytometry. Weri-Rb1 or Y79 cells were seeded at a density of $1x10^4$ cells/well in 96-well plates. In brief, cells were transfected with si-H19 or si-NC as aforementioned and, 2 days post-transfection, cells were trypsinized by 0.25% Trypsin (Gibco; Thermo Fisher Scientific, Inc.), followed by centrifugation at 350 x g for 2 min. and washed with PBS. Cells were then resuspended in PBS and fixed with 100% ethanol at 4˚C overnight, and apoptosis was detected using a dual-staining method with annexin V-fluorescein isothiocyanate in combination with propidium iodide (D Pharmingen, San Diego, CA, USA). Apoptosis was analyzed using a FACScan flow cytometer and Cell Quest analysis software version 5.2 (BD Biosciences, Franklin Lakes, NJ, USA). Each experiment was run in quadruplicate for each condition.

Cell proliferation analysis. Weri-Rb1 or Y79 cells were transfected with si-H19 or si-NC for 24 h, and then seeded in 6-well plate with a density of $0.5x10^3$ cells per well and cultured for 7-10 days with RPMI-1640 medium (Gibco; Thermo Fisher Scientific, Inc.) supplemented with 10% FBS, 100 U/ml penicillin (Invitrogen, Thermo Fisher Scientific, Inc.), and 100 mg/ml streptomycin (Invitrogen, Thermo Fisher Scientific, Inc.). The medium was replenished every two days. Colonies were then fixed for 5 min at room temperature with 10% formaldehyde, stained with 1.0% crystal violet for 30 sec at room

temperature and counted under a light microscope (Olympus, Tokyo, Japan) in five predetermined fields of interest at x200 magnification. An MTT assay was performed using the Cell Proliferation kit I (Roche Diagnostics, Basel, Switzerland) according to the manufacturer's protocol. Briefly, 0.5 mg/ml MTT and 100% dimethylsulfoxide reagent were added to the cells at the indicted times. The optical density was measured at 590 nm using the Tecan SpectraFluor Microplate Reader (Tecan Group, Ltd., Mannedorf, Switzerland). Experiments were performed three times.

Cell migration and invasion assays. Cell migration and invasion assays were performed using Transwell insert chambers (Costar; Corning Incorporated, Corning, NY, USA), In brief, Weri-Rb1 or Y79 cells were seeded at a density of $1x10^4$ cells/100 ml RPMI-1640 medium, without FBS, on a fibronectin-coated polycarbonate membrane insert in a Transwell apparatus (Costar; Corning Incorporated) and the lower chamber was filled with 500 μl RPMI-1640 medium (Gibco; Thermo Fisher Scientific, Inc.) supplemented with 20% FBS, 100 U/ml penicillin (Invitrogen, Thermo Fisher Scientific, Inc.), and 100 mg/ml streptomycin (Invitrogen, Thermo Fisher Scientific, Inc.). Cells were incubated for 12 h at 37˚C in a humidified atmosphere containing 5% CO_2. And then the cells adhering to the lower surface were fixed with 100% methanol for 10 min at room temperature, stained with Giemsa solution at room temperature for 10 min and washed with PBS three times. The cells colonies were then counted under a light microscope (Olympus Corporation, Tokyo, Japan) in five predetermined fields of interest at x200 magnification. The cell invasion assay was performed as aforementioned, with the exception that the Transwell membranes were precoated with 24 mg/ml Matrigel (R&D Systems, Inc., Minneapolis, MN, USA). Cells were counted as aforementioned. Experimental data are representative of a minimum of three independent repeats.

In vivo growth assay. A total of 40 female nude mice (18-20 g, Balb/C-nu/nu athymic; 4-5 weeks old) were purchased from the Animal Center of the Cancer Institute of Chinese Academy of Medical Science (Beijing, China). The mice were maintained in a facility under specific pathogen-free conditions and an allowed free access to pathogen free laboratory chow, allowed free access to autoclaved water in an air-conditioned room with a 12 h light/dark cycle. Mice were divided into an si-H19 group and an si-NC group (with each group containing 20 mice). Suspensions of $1x10^7$ cells (Y79 cells transfected with siRNA duplexes) were subcutaneously injected into the upper back of the female nude mice. Mice were monitored daily. Tumor samples were carefully removed 21 days after injection and the size was calculated on the basis of width (x) and length (y): $x^2y/2$, where $x<y$. The humane endpoints for the present study was that the mean diameter of the tumor did not exceed 1.2 cm in mice. Ethical approval for the animal experiments was granted by the Animal Ethical and Welfare Committee of Tianjin Medical University (Tianjin, China).

Western blotting. Total protein was extracted from transfected cells with radioimmunoprecipitation lysis buffer (http://www.keygentec.com.cn/; KenGEN, Nanjing, Jiangsu, China) for 30 min at 4˚C, and centrifuged at 12,000 x g for 10 min at 4˚C. The supernatant fraction was collected and then quantified using a bicinchoninic acid protein assay kit (Beyotime Institute of Biotechnology, Haimen, China). Protein lysates (30 mg) were separated by 12% SDS-PAGE and transferred onto polyvinylidene difluoride membranes (Merck KGaA, Darmstadt, Germany) at 30 V overnight. The membranes were blocked with 5% non-fat milk in TBST for 1 h at room temperature and gentle shaking, and then probed with antibodies against epithelial (E-)cadherin (cat. no. ab15148, dilution 1:1,000; Abcam, Cambridge, UK), MMP9 (cat. no. sc-10737, dilution 1:200; Santa Cruz Biotechnology, Inc., Dallas, TX, USA), CDH13 (cat. no. sc-7940, dilution 1:200; Santa Cruz Biotechnology, Inc.), vimentin (cat. no. sc-5565, dilution 1:300; Santa Cruz Biotechnology, Inc.) and GAPDH (cat. no. sc-25778, dilution 1:2,500; Santa Cruz Biotechnology, Inc.) at 4˚C overnight. Following washing 3 times with TBS 0.1% Tween 20, the membranes were incubated with goat anti-rabbit horseradish peroxidase-conjugated secondary antibody (cat. no. 7074, Cell Signaling Technology, Danvers, MA, USA) at a dilution of 1:5,000 for 1 h at room temperature. Band detection was performed using an enhanced chemiluminescence kit (Pierce; Thermo Fisher Scientific, Inc.), according to the manufacturer's protocol.

Statistical analysis. Statistical analyses were performed using the SPSS software package 17.0 (SPSS, Inc., Chicago, IL, USA). Results are expressed as the mean ± standard deviation. Data analysis was performed using Student's t-test (two-tailed) and one-way-analysis of variance followed by Tukey's multiple comparisons test as a post-hoc test. Univariate and multivariate relative risks were calculated using the Cox proportional hazards regression. $P<0.05$ was considered to indicate a statistically significant difference.

Results

lncRNAH19 is overexpressed in retinoblastoma tissues and cell lines. To explore whether lncRNA *H19* had an effect on the malignant phenotype of retinoblastoma, the expression pattern of *H19* in retinoblastoma tissues and cell lines was analyzed. The results from the present study indicated that *H19* expression was significantly increased in retinoblastoma tissues compared with non-tumor retinal tissues ($P<0.001$; Fig. 1A). In addition, lncRNA *H19* expression was upregulated in Weri-Rb1 and Y79 retinoblastoma cells compared with ARPE-19 and HRMECs ($P<0.05$; Fig. 1B).

lncRNA H19 is associated with retinoblastoma progression. To investigate the association between lncRNA *H19* and retinoblastoma further, the overall survival times of patients with retinoblastoma were analyzed in accordance with *H19* expression levels. According to classification by Motoyama *et al* (23), 80 retinoblastoma tissue samples were divided into the high-expression group (n=38) or the low-expression group (n=42). As presented in Table I, the associations between lncRNA *H19* expression and tumor size (<10 vs. ≥10 mm; $P=0.007$), optic nerve invasion (positive vs. negative; $P=0.013$) and choroidal invasion (positive vs. negative; $P=0.043$) were statistically significant. However, no significant associations

Table I. Association between lncRNA *H19* expression and clinicopathological characteristics in retinoblastoma.

Characteristic	Number	lncRNA *H19* expression		P-value
		High	Low	
Age, years				
<2	40	22 (55)	18 (45)	0.263
≥2	40	16 (40)	24 (60)	
Sex				
Male	44	18 (40.9)	26 (59.1)	0.750
Female	36	16 (44.4)	20 (55.6)	
Tumor size, mm				
<10	33	11 (33.3)	22 (66.7)	0.007[a]
≥10	47	30 (63.8)	17 (36.2)	
Choroidal invasion				
Negative	45	18 (40)	27 (60)	0.043[a]
Positive	35	22 (62.9)	13 (37.1)	
Optic nerve invasion				
Negative	47	26 (55.3)	31 (44.7)	0.013[a]
Positive	43	24 (72.7)	9 (27.3)	
Laterality				
Unilateral	56	27 (48.2)	29 (51.8)	0.626
Bilateral	24	13 (54.2)	11 (45.8)	
Pathological grade				
Well-differentiated	43	24 (55.8)	19 (44.2)	0.282
Poorly	37	25 (67.6)	12 (32.4)	

[a]P<0.05.

in age (P=0.263), sex (P=0.750), laterality (P=0.626) or pathological grade (P=0.282) were observed. Overall survival analysis demonstrated that the level of lncRNA *H19* expression was significantly associated with the overall survival rate of retinoblastoma patients, as patients with high lncRNA *H19* levels had a poorer survival rate compared with those with low lncRNA *H19* levels (P<0.001; Fig. 1C). Simultaneously, multivariate analysis was applied to evaluate the association between lncRNA *H19* expression and prognostic factors for overall survival rates. The results presented in Table II demonstrated that increased lncRNA *H19* expression was a poor independent prognostic factor for patients with retinoblastoma (P<0.040).

Knockdown of lncRNA H19 decreases retinoblastoma cell proliferation. To elucidate the function of *H19* on retinoblastoma cell proliferation, loss-of-function analysis using retroviral transduction of *H19* in Weri-Rb1 and Y79 cells was performed. qPCR analysis was performed to confirm that *H19* expression was significantly inhibited following knockdown (Fig. 2A). The MTT assay results revealed that the viability of cells (Weri-Rb1 and Y79 cells) transfected with si-H19 was significantly decreased compared with controls, at 48- and 72 h post-transfection (Fig. 2B and C). In addition, the results of the cell colony assay demonstrated that inhibition of *H19* expression resulted in decreased cell proliferation in Weri-Rb1 and Y79 cells compared with controls (Fig. 2D).

Knockdown of lncRNA H19 promotes cell apoptosis. As aforementioned, knocking down *H19* significantly decreased retinoblastoma cell proliferation, and therefore the subsequent effects on cell cycle and apoptosis were investigated further. In accordance with the aforementioned results, cells transfected with si-H19 displayed an increased proportion of G_1 phase cells and a decreased proportion of S phase cells, indicating that silencing *H19* may induce G_1/S phase arrest in Weri-Rb1 and Y79 cells (Fig. 3A). Furthermore, analysis of cell apoptosis in the si-H19 group was markedly increased compared with si-NC (P<0.05; Fig. 3B). Consistent with these changes, the expression of apoptosis-associated proteins, including cyclin D1, Bax and p53 was decreased in the si-H19 group compared with that in the si-NC group (Fig. 3C), which indicated that *H19* may influence cell apoptosis in Weri-Rb1 and Y79 cells.

Knockdown of lncRNAH19 inhibits cells migration and invasion in vitro. The effect of lncRNA *H19* on cell migration and invasion in Y79 cells was investigated further. The results of the present study of the Matrigel invasion assay revealed that the number of migratory cells in the si-H19 group was significantly decreased compared with that in the si-NC group (P<0.05; Fig. 4A). As presented in Fig. 4B, the migration of cells transfected with si-H19 was also significantly suppressed in Y79 cells (P<0.05; Fig. 4B). Taken together, these results support the hypothesis that silencing of lncRNA *H19* inhibited the migration and invasion of Y79 cells. In addition, the effects of lncRNA *H19* on the expression of the migration- and invasion-associated proteins MMP9, CDH13, E-cadherin and vimentin were analyzed. As presented in Fig. 4C, lncRNA *H19* downregulation decreased the expression of MMP9, CDH13, vimentin and E-cadherin compared with that in the si-NC group.

Knockdown of lncRNA H19 suppresses the proliferation of retinoblastoma cells in vivo. To validate the effects of lncRNA *H19* on the proliferation and invasion of Y79 cells *in vivo*, the volume of tumors that grew in a nude mice xenograft model, 3 weeks after subcutaneous injection of Y79/si-H19 cells, were analyzed. After 3 weeks, subcutaneous tumors were established in the right groin of 20 nude mice injected with Y79/si-H19 or Y79/si-NC cells. Furthermore, a significant decrease in tumor volume was only observed in the si-H19 treatment group, compared with corresponding controls (Y79/si-NC cells). The results of the present study demonstrated that lncRNA *H19* inhibited the proliferation of retinoblastoma cells *in vivo*.

Discussion

LncRNAs, >200 nucleotides in length, are intergenic transcripts, which, although they do not exhibit a protein-coding function, have been identified to mediate structural and regulatory functions in the development and pathogenesis of cancer (24-26). It is well-documented that lncRNAs exert regulatory functions via interactions with target genes, cell

Table II. Univariate and multivariate Cox's regression of prognostic factors for overall survival in retinoblastoma.

	Univariate analysis			Multivariate analysis		
Characteristic	HR	95% CI	P-value	HR	95% CI	P-value
Age, years						
<2 vs. ≥2	1.046	0.425-2.433	0.875			
Sex						
Male vs. female	1.204	0.569-2.364	0.640			
Size, mm						
<10 vs. ≥10	5.012	2.011-12.04	0.001[a]	2.01	0.715-7.140	0.249
Choroidal invasion						
Negative vs. positive	4.497	1.978-10.013	<0.001[a]	1.848	0.695-4.827	0.213
Optic nerve invasion						
Negative vs. positive	4.098	1.457-5.98	0.001[a]	3.126	1.321-6.015	0.038[a]
Laterality						
Bilateral vs. unilateral	1.654	0.871-2.923	0.397			
Pathological grade						
Well-differentiated vs. poorly	0.818	0.353-1.857	0.270			
LncRNA-*H19*						
Low vs. high	5.124	2.324-11.532	<0.001[a]	2.912	1.021-8.452	0.039[a]

[a]P<0.05; HR, hazard ratio; CI, confidence interval.

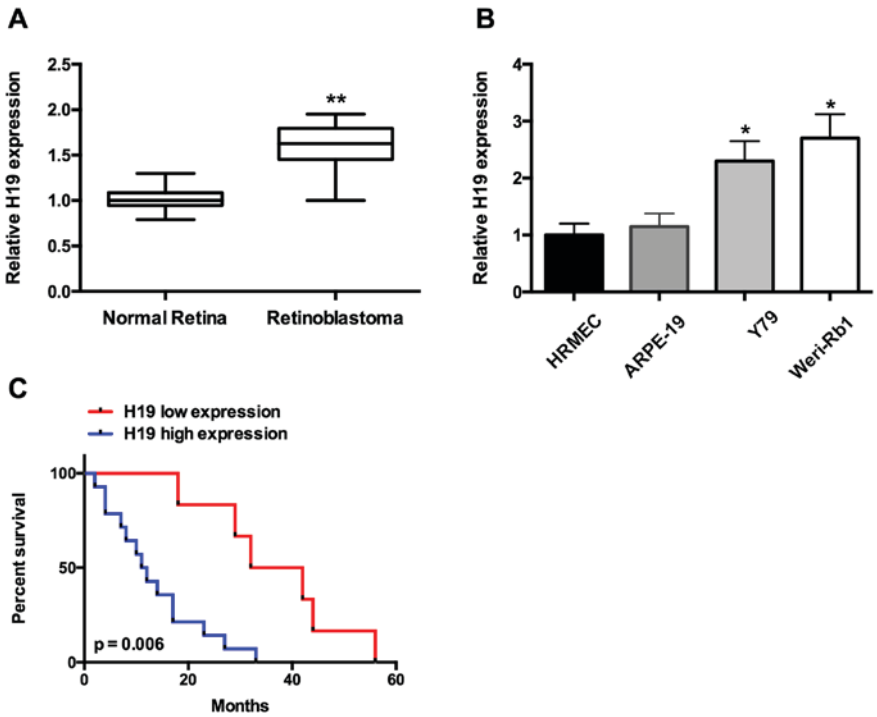

Figure 1. Expression of lncRNA-*H19* in retinoblastoma tissues and cell lines, and overall survival rates in patients with retinoblastoma. (A) Expression of lncRNA-*H19* is increased in retinoblastoma tissues (B) Expression of lncRNA-*H19* is increased in Weri-Rb1 and Y79 cells (C) Kaplan-Meier estimator analysis and log-rank test to assess the association between lncRNA-*H19* expression and survival rates of patients with retinoblastoma. *P<0.05, **P<0.001 vs. normal retina. lncRNA-*H19*, long non-coding RNA-*H19*.

cycle regulators, transcription factors or chromatin-modifying complexes, including p53 (27), E2Fs (28), Enhancer of Zeste homolog 2 (29) and sex-determining region y-related high-mobility group-box-2 (30). It has been identified that

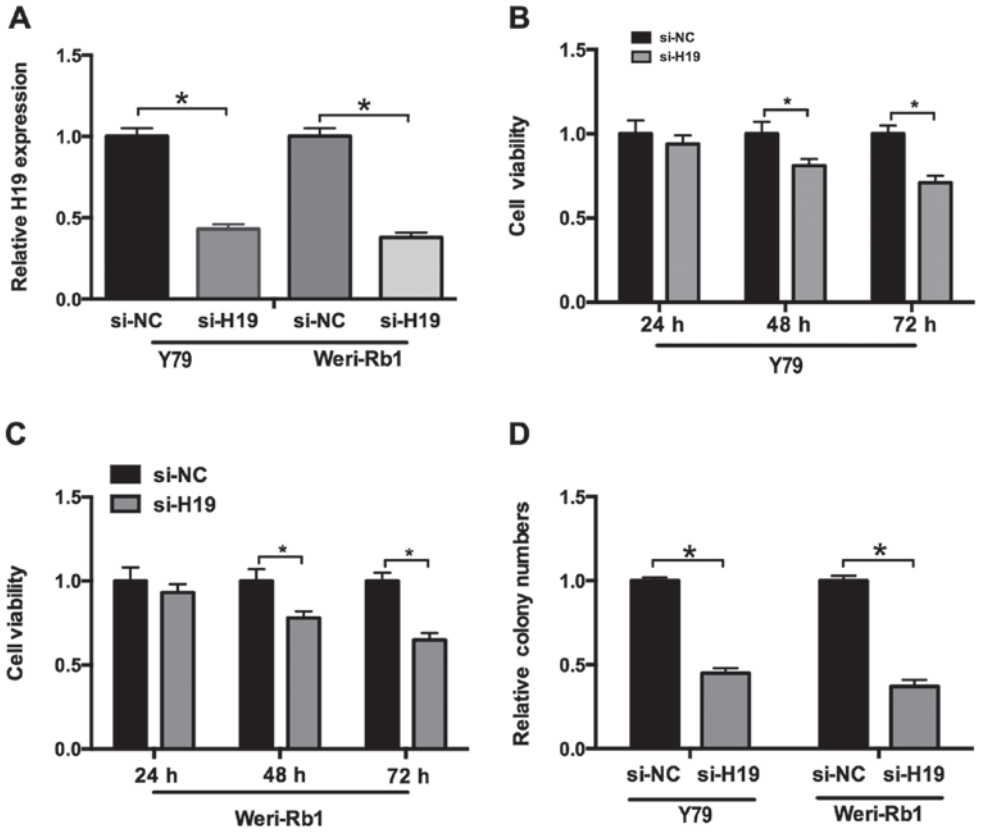

Figure 2. Knockdown of *H19* by si-H19 significantly suppresses retinoblastoma cell viability and colony numbers in Y79 and Weri-Rb1 cells. (A) Expression of lncRNA-*H19* is decreased in Y79 and Weri-Rb1 cell lines transfected with si-H19. Cell viability is repressed in (B) Y79 and (C) Weri-Rb1 cells, 48 and 72 h post-transfection with si-H19. (D) Colony numbers are decreased in Y79 and Weri-Rb1 cells post-transfection with si-H19. *P<0.05 vs. si-NC. si-H19, *H19*-specific short interfering RNA; lncRNA-*H19*, long non-coding RNA-*H19*; si-NC, negative control short interfering RNA.

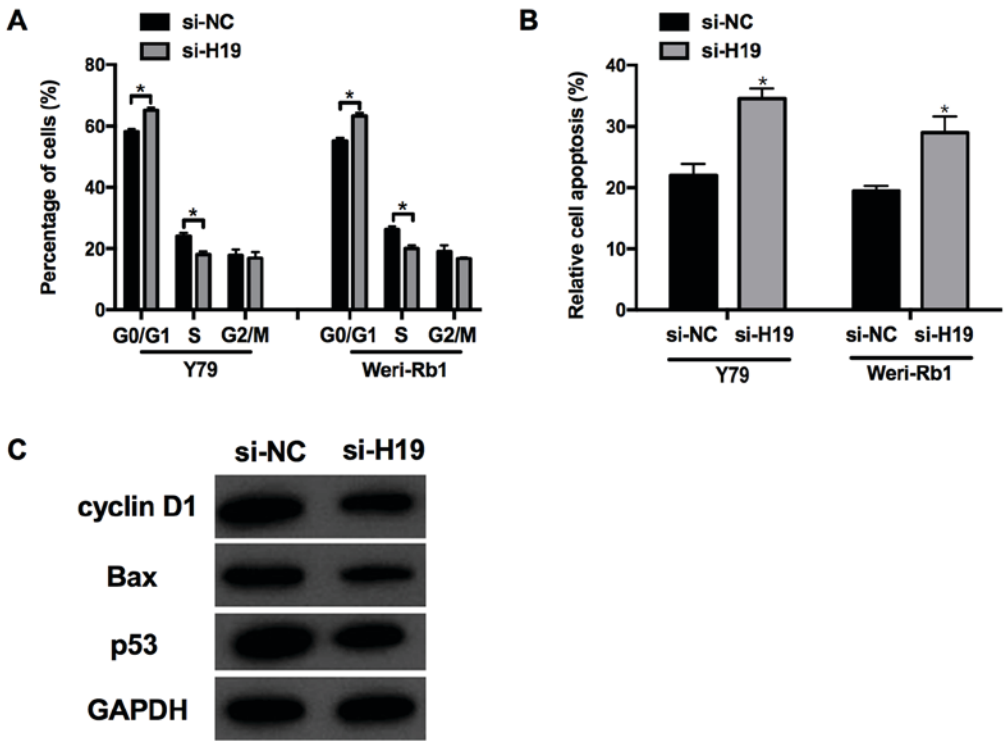

Figure 3. Effects of lncRNA-*H19* on cell cycle and apoptosis. Effects of lncRNA-*H19* knockdown on (A) cell cycle and (B) apoptosis of Weri-Rb1 and Y79 cells analyzed by flow cytometry. (C) Western blot analysis of CDK1, Bax and p53 protein expression in Y79 cells transfected with si-H19. *P<0.05 vs. si-NC. lncRNA-*H19*, long non-codingRNA-*H19*; CDK1, cyclin-dependent kinase 1; Bax, B-cell lymphoma 2-associated X protein; si-H19, *H19*-specific short interfering RNA; si-NC, negative control short interfering RNA.

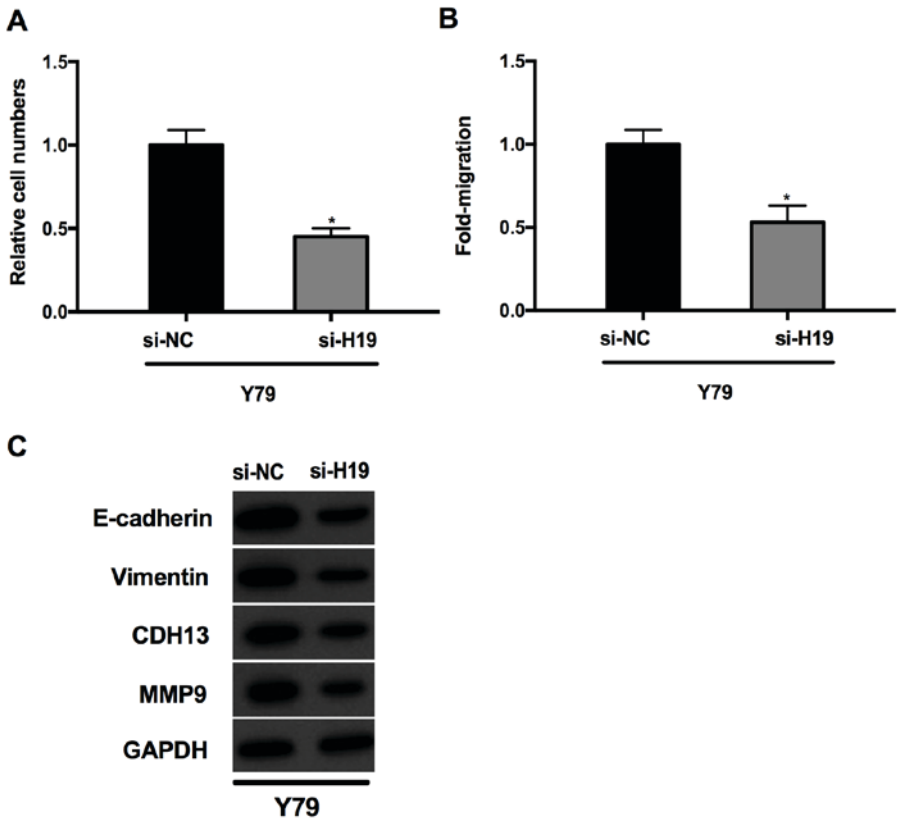

Figure 4. Effect of lncRNA-*H19* silencing on the migration and invasion of Y79 cells. Effects of lncRNA-*H19* knockdown on (A) numbers and (B) migration of Y79 cells *in vitro*. (C) Western blot analysis of E-cadherin, vimentin, CDH13 and MMP9 protein expression in Y79 cells following lncRNA-*H19* knockdown. *P<0.05 vs. si-NC. si-H19, *H19*-specific short interfering RNA; si-NC, negative control short interfering RNA; lncRNA-*H19*, long non-coding RNA-*H19*; CDH13, cadherin 13; MMP9, matrix metalloproteinase 9.

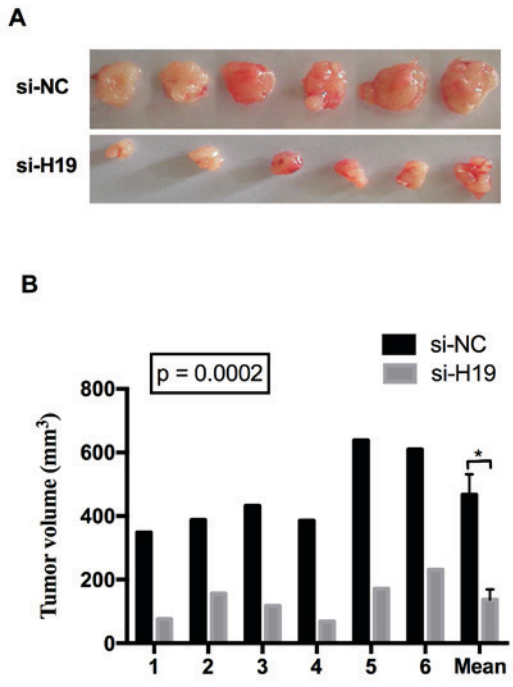

Figure 5. Tumors isolated from mice post-injection with Y79/si-H19 or Y79/si-NC cells. (A) Subcutaneous tumors established in the right groin of five nude mice injected with Y79/si-H19 or Y79/si-NC cells. (B) Quantification of average tumor volumes. *P<0.05, where P=0.0002, indicating the means of 6 tumors in si-NC group compared with that in the si-H19 group, and, *H19*-specific short interfering RNA; si-NC, negative control short interfering RNA.

aberrant lncRNA expression is associated with multiple diverse cancer processes, indicating that lncRNAs may have a marked function in cancer development. A well-documented lncRNA, namely E2F1-regulated inhibitor of cell death (*ERIC*) was transcriptionally upregulated upon activation, and inhibition of *ERIC* resulted in increased apoptotic cell death (31).

Previous studies have demonstrated that lncRNA-*H19* is involved in the development of cancer pathogenesis and may serve as a potential tumor biomarker. For example, Luo *et al* (32) observed that the *H19* expression pattern was markedly increased in patients with invasive bladder cancer and demonstrated pro-tumorigenic properties. Furthermore, the level of *H19* was significantly upregulated in patients with gastric cancer (GC), and the increased expression promoted the differentiation of early-stage GC (33). Shi *et al* (18) also revealed that *H19* expression was associated with tumor grade, and was able to mediate glioma cell invasion by directly regulating CDH13. Consistent with previous studies, the present study demonstrated that *H19* levels were markedly increased in retinoblastoma cells and tissues, and may serve a crucial function in retinoblastoma migration and invasion, as a potential novel target for therapeutic strategy and prognostic prediction.

In order to investigate the function of *H19* further, an *in vivo* murine model in which female nude mice were injected with Y79/si-H19 cells was established. At 3 weeks post-injection, mice exhibited subcutaneous tumors and tumor volumes were significantly decreased in the si-H19 treatment group compared with controls, indicating that *H19* may be

involved in the development of retinoblastoma. Furthermore, the survival rates of patients with retinoblastoma with varying *H19* expression levels were determined, and it was revealed that patients with high *H19* levels had a poorer survival rate compared with those with low *H19* levels. Therefore, the results of the present study indicated that patients with high *H19* levels had a shorter survival time compared with patients with low levels. Collectively, the results support the hypothesis that *H19* knockdown significantly increased the proliferation and inhibited the apoptosis of retinoblastoma cells.

Previous studies have demonstrated that ectopic expression of *H19* partly contributed to increased cell proliferation, cancer migration and invasion by targeting miRNA (18,19). The results of the present study demonstrated that *H19* promoted the proliferation, migration and invasion of Weri-Rb1 and Y79 cells, whereas silencing *H19* significantly suppressed cell proliferation, migration and invasion *in vitro*. Furthermore, *H19* regulates several proteins, including vimentin, CDK1, p53, CDH13 and E-cadherin. For example, *H19* functioned as a competing endogenous RNA for miR-138 and miR-200a, antagonized their functions and led to the de-repression of their endogenous targets vimentin, E-cadherin and CDH13 (18,32,34,35). In the present study, the expression pattern of several corresponding proteins was investigated, and it was revealed that inhibition of *H19* repressed MMP9, CDH13, vimentin and E-cadherin expression. However, the precise association between *H19* and the corresponding proteins requires further study.

In conclusion, the results of the present study indicated that *H19* may serve an oncogenic function in retinoblastoma cells and tissues, suggesting that inhibition of *H19* may be a potential target mechanism for retinoblastoma therapy.

Acknowledgements

Not applicable.

Funding

The present study was supported by the Foundation of Premature Retinopathy Genetic Screening and Clinical Screening Study (grant no. 2011KR17).

Availability of data and materials

The data generated in the present study are available from the corresponding author upon reasonable request.

Author's contributions

LL and LST performed the experiment. WC and YCW analyzed the experimental data and patients data. MH designed the experiment and wrote the manuscript. All authors read and approved the final manuscript.

Ethics approval and consent to participate

The present study was approved by the Research Ethics Committee of Tianjin Eye Hospital (Tianjin, China) and written informed consent was obtained from all patients.

Consent for publication

Written informed consent was obtained from all patients.

Competing interests

The authors declare that they have no competing interests.

References

1. Villegas VM, Hess DJ, Wildner A, Gold AS and Murray TG: Retinoblastoma. Curr Opin Ophthalmol 24: 581-588, 2013.
2. American Cancer Society: Learn about cancer. Retinoblastoma. https://www.cancer.org/cancer/retinoblastoma.html.
3. Hernando E, Nahlé Z, Juan G, Diaz-Rodriguez E, Alaminos M, Hemann M, Michel L, Mittal V, Gerald W, Benezra R, *et al*: Rb inactivation promotes genomic instability by uncoupling cell cycle progression from mitotic control. Nature 430: 797-802, 2004.
4. Dimaras H, Khetan V, Halliday W, Orlic M, Prigoda NL, Piovesan B, Marrano P, Corson TW, Eagle RC Jr, Squire JA and Gallie BL: Loss of RB1 induces non-proliferative retinoma: Increasing genomic instability correlates with progression to retinoblastoma. Hum Mol Genet 17: 1363-1372, 2008.
5. Manning AL, Longworth MS and Dyson NJ: Loss of pRB causes centromere dysfunction and chromosomal instability. Genes Dev 24: 1364-1376, 2010.
6. Amato A, Lentini L, Schillaci T, Iovino F and Di Leonardo A: RNAi mediated acute depletion of retinoblastoma protein (pRb) promotes aneuploidy in human primary cells via micronuclei formation. BMC Cell Biol 10: 79, 2009.
7. Iovino F, Lentini L, Amato A and Di Leonardo A: RB acute loss induces centrosome amplification and aneuploidy in murine primary fibroblasts. Mol Cancer 5: 38, 2006.
8. Lin P and O'Brien JM: Frontiers in the management of retinoblastoma. Am J Ophthalmol 148: 192-198, 2009.
9. Dalgard CL, Gonzalez M, deNiro JE and O'Brien JM: Differential microRNA-34a expression and tumor suppressor function in retinoblastoma cells. Invest Ophthalmol Vis Sci 50: 4542-4551, 2009.
10. Tsai MC, Spitale RC and Chang HY: Long intergenic noncoding RNAs: New links in cancer progression. Cancer Res 71: 3-7, 2011.
11. Wapinski O and Chang HY: Long noncoding RNAs and human disease. Trends Cell Biol 21: 354-361, 2011.
12. Carninci P, Kasukawa T, Katayama S, Gough J, Frith MC, Maeda N, Oyama R, Ravasi T, Lenhard B, Wells C, *et al*: The transcriptional landscape of the mammalian genome. Science 309: 1559-1563, 2005.
13. Spizzo R, Almeida MI, Colombatti A and Calin GA: Long non-coding RNAs and cancer: A new frontier of translational research? Oncogene 31: 4577-4587, 2012.
14. Adriaenssens E, Dumont L, Lottin S, Bolle D, Leprêtre A, Delobelle A, Bouali F, Dugimont T, Coll J and Curgy JJ: H19 overexpression in breast adenocarcinoma stromal cells is associated with tumor values and steroid receptor status but independent of p53 and Ki-67 expression. Am J Pathol 153: 1597-1607, 1998.
15. Cooper MJ, Fischer M, Komitowski D, Shevelev A, Schulze E, Ariel I, Tykocinski ML, Miron S, Ilan J, de Groot N and Hochberg A: Developmentally imprinted genes as markers for bladder tumor progression. J Urol 155: 2120-2127, 1996.
16. Lottin S, Adriaenssens E, Dupressoir T, Berteaux N, Montpellier C, Coll J, Dugimont T and Curgy JJ: Overexpression of an ectopic H19 gene enhances the tumorigenic properties of breast cancer cells. Carcinogenesis 23: 1885-1895, 2002.
17. Biran H, Ariel I, de Groot N, Shani A and Hochberg A: Human imprinted genes as oncodevelopmental markers. Tumour Biol 15: 123-134, 1994.
18. Shi Y, Wang Y, Luan W, Wang P, Tao T, Zhang J, Qian J, Liu N and You Y: Long non-coding RNA H19 promotes glioma cell invasion by deriving miR-675. PLoS One 9: e86295, 2014.
19. Yang F, Bi J, Xue X, Zheng L, Zhi K, Hua J and Fang G: Up-regulated long non-coding RNA H19 contributes to proliferation of gastric cancer cells. FEBS J 279: 3159-3165, 2012.

20. Matouk IJ, Raveh E, Abu-lail R, Mezan S, Gilon M, Gershtain E, Birman T, Gallula J, Schneider T, Barkali M, *et al*: Oncofetal H19 RNA promotes tumor metastasis. Biochim Biophys Acta 1843: 1414-1426, 2014.
21. Hibi K, Nakamura H, Hirai A, Fujikake Y, Kasai Y, Akiyama S, Ito K and Takagi H: Loss of H19 imprinting in esophageal cancer. Cancer Res 56: 480-482, 1996.
22. Livak KJ and Schmittgen TD: Analysis of relative gene expression data using real-time quantitative PCR and the 2(-Delta Delta C(T)) method. Methods 25: 402-408, 2001.
23. Motoyama K, Inoue H, Nakamura Y, Uetake H, Sugihara K and Mori M: Clinical significance of high mobility group A2 in human gastric cancer and its relationship to let-7 microRNA family. Clin Cancer Res 14: 2334-2340, 2008.
24. Mattick JS and Gagen MJ: The evolution of controlled multitasked gene networks: The role of introns and other noncoding RNAs in the development of complex organisms. Mol Biol Evol 18: 1611-1630, 2001.
25. Gibb EA, Brown CJ and Lam WL: The functional role of long non-coding RNA in human carcinomas. Mol Cancer 10: 38, 2011.
26. Gibb EA, Vucic EA, Enfield KS, Stewart GL, Lonergan KM, Kennett JY, Becker-Santos DD, MacAulay CE, Lam S, Brown CJ and Lam WL: Human cancer long non-coding RNA transcriptomes. PLoS One 6: e25915, 2011.
27. Huarte M, Guttman M, Feldser D, Garber M, Koziol MJ, Kenzelmann-Broz D, Khalil AM, Zuk O, Amit I, Rabani M, *et al*: A large intergenic noncoding RNA induced by p53 mediates global gene repression in the p53 response. Cell 142: 409-419, 2010.
28. Polager S and Ginsberg D: E2F-at the crossroads of life and death. Trends Cell Biol 18: 528-535, 2008.
29. Zhao J, Sun BK, Erwin JA, Song JJ and Lee JT: Polycomb proteins targeted by a short repeat RNA to the mouse X chromosome. Science 322: 750-756, 2008.
30. Amaral PP, Neyt C, Wilkins SJ, Askarian-Amiri ME, Sunkin SM, Perkins AC and Mattick JS: Complex architecture and regulated expression of the SOX2ot locus during vertebrate development. RNA 15: 2013-2027, 2009.
31. Feldstein O, Nizri T, Doniger T, Jacob J, Rechavi G and Ginsberg D: The long non-coding RNA ERIC is regulated by E2F and modulates the cellular response to DNA damage. Mol Cancer 12: 131, 2013.
32. Luo M, Li Z, Wang W, Zeng Y, Liu Z and Qiu J: Long non-coding RNA H19 increases bladder cancer metastasis by associating with EZH2 and inhibiting E-cadherin expression. Cancer Lett 333: 213-221, 2013.
33. Zhou X, Yin C, Dang Y, Ye F and Zhang G: Identification of the long noncoding RNA H19 in plasma as a novel biomarker for diagnosis of gastric cancer. Sci Rep 5: 11516, 2015.
34. Liang WC, Fu WM, Wong CW, Wang Y, Wang WM, Hu GX, Zhang L, Xiao LJ, Wan DC, Zhang JF and Waye MM: The lncRNA H19 promotes epithelial to mesenchymal transition by functioning as MiRNA sponges in colorectal cancer. Oncotarget 6: 22513-22525, 2015.
35. Wan X, Ding X, Chen S, Song H, Jiang H, Fang Y, Li P and Guo J: The functional sites of miRNAs and lncRNAs in gastric carcinogenesis. Tumor Biol 36: 521-532, 2015.